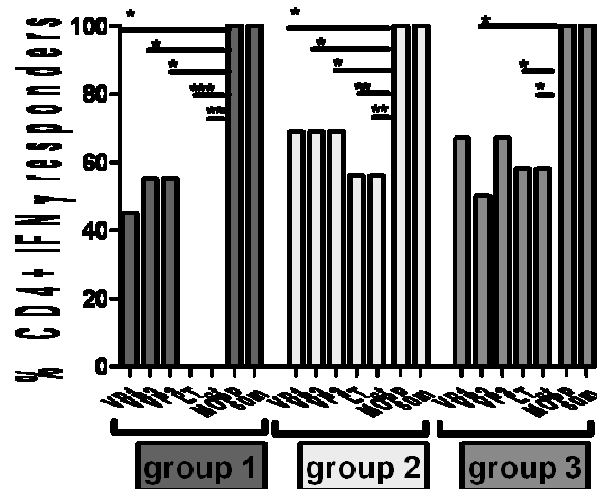


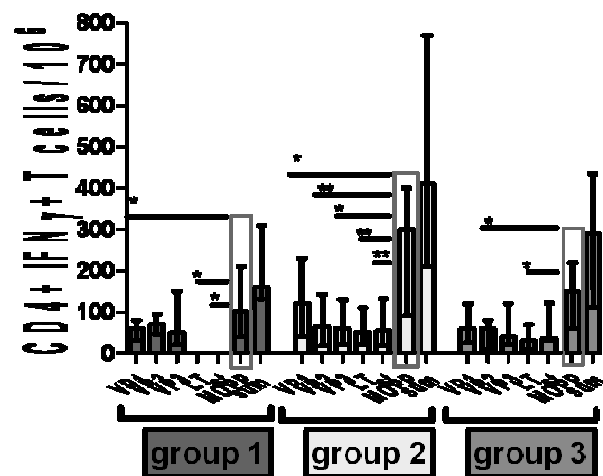
Supplemental Digital Content 1

(SDC 1) – Combined SDC File

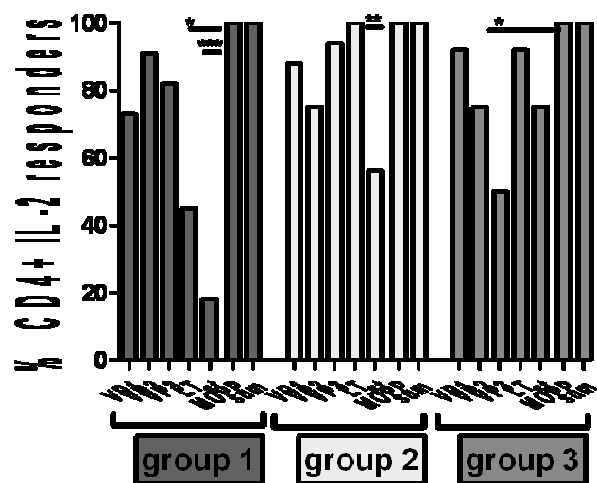
A



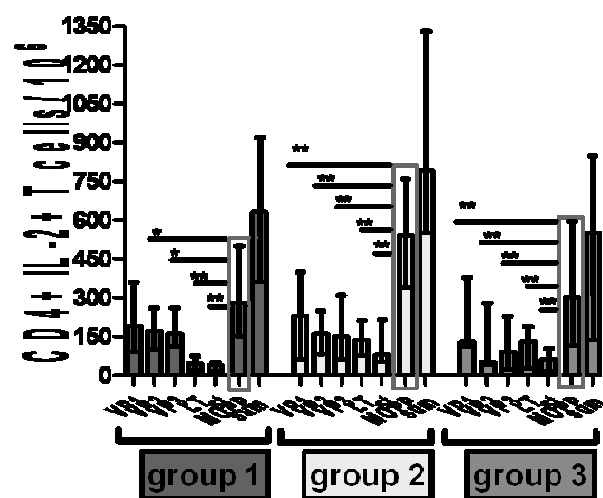
B



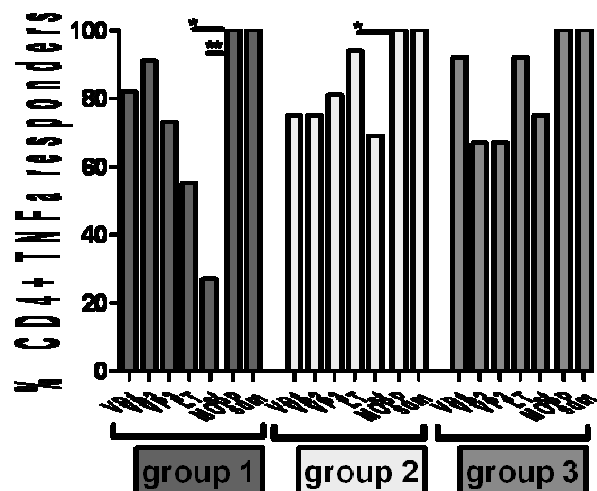
C



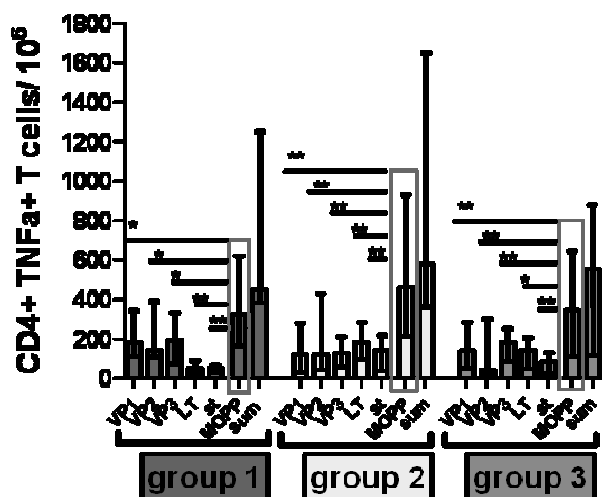
D



E



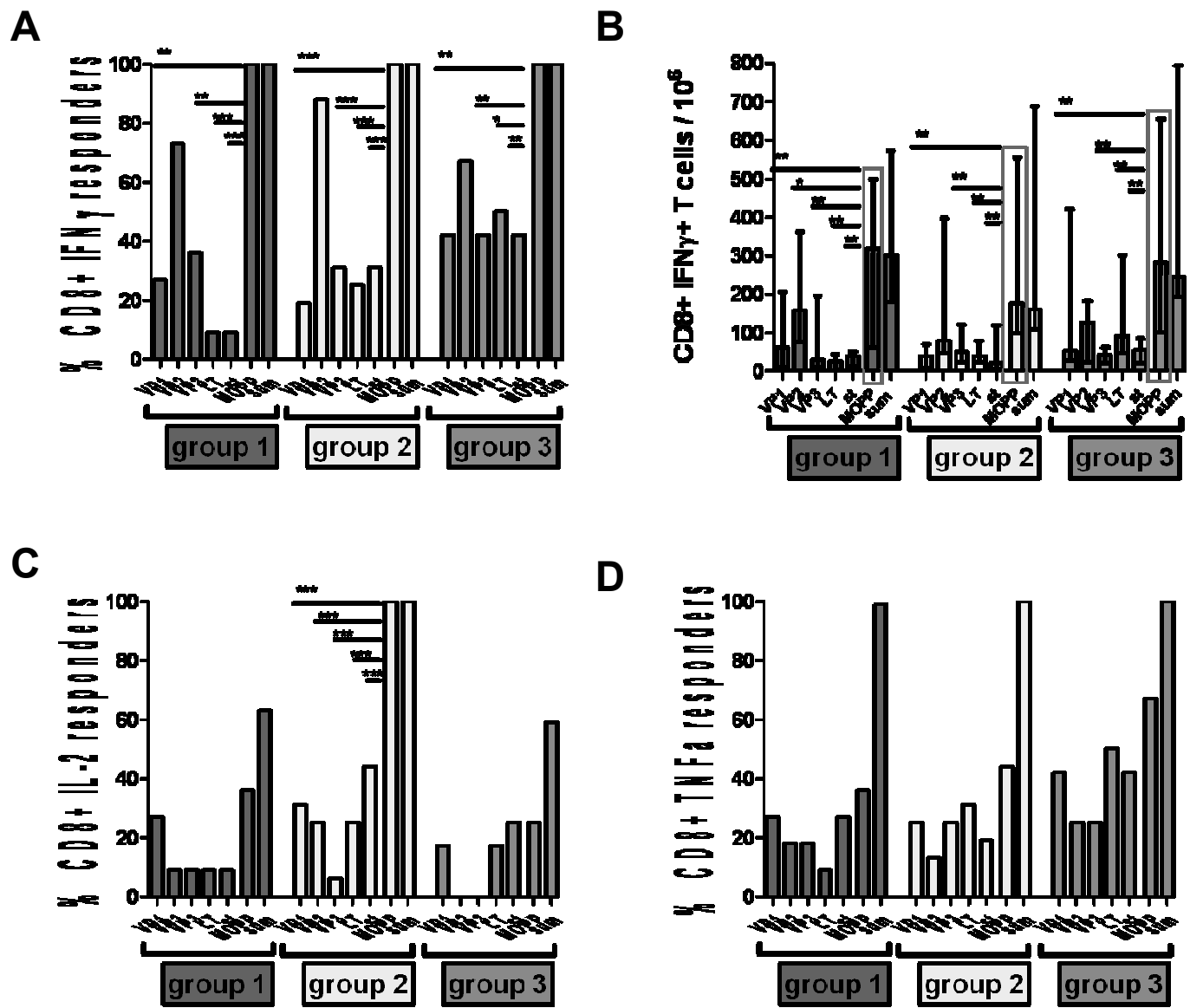
F



Supplemental Figure 1

Supplemental Figure S1. Incidence of CD4+ IFN γ (A), IL-2 (C) and TNFa (E) responders and magnitude of total IFN γ + (B), IL-2+ (D) and TNFa+ (F) CD4+ T-cell responses in different patient groups

Figures A, C, D demonstrate the percentage of KTRs with detectable SOPP (VP1, VP2, VP3, LT, or st, respectively)-specific versus MOPP and theoretical summated response (sum)-specific IFN γ -, IL-2- and TNFa-producing CD4+ T-cells, respectively. Figures B, D, F show the median frequencies with inter-quartile range of BKV-specific CD4+ T cells that produce IFN γ , IL-2 and TNFa, respectively upon VP1-, VP2-, VP3-, LT-, st- single stimulation (SOPP) in comparison with MOPP and sum stimulation and after background subtraction. Stimulation with MOPP showed a higher percentage of patients with detectable BKV-specific CD4+ T-cells in all patient groups and a significantly higher magnitude of T-cell responses (* $p < 0.05$; ** $p < 0.01$; *** $p < 0.001$). The higher magnitude of T-cell responses obtained from the calculated theoretical sum versus MOPP reflects the amino acid overlap within regulatory proteins LT and st and structural proteins VP1, VP2, VP3, respectively.

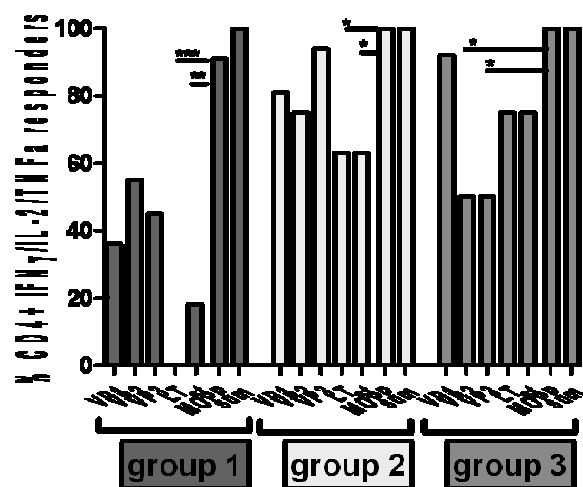


Supplemental figure 2

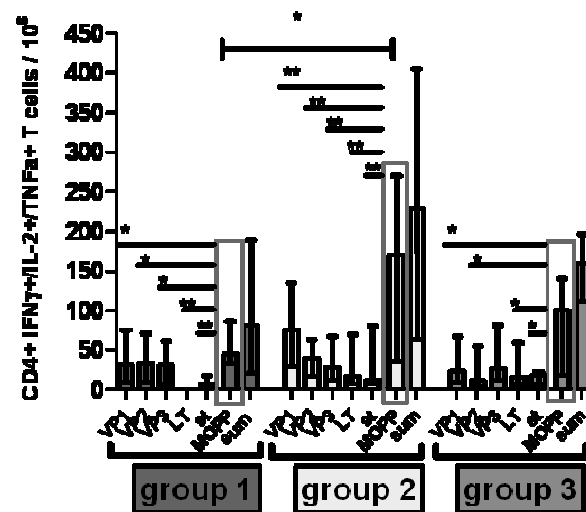
Supplemental Figure S2. Incidence of CD8+ IFN γ (A), IL-2 (C) and TNF α (D) responders and magnitude of total IFN γ + (B) CD8+ T-cell responses in different patient groups

Figures A, C, D demonstrate the percentage of KTRs with detectable SOPP (VP1, VP2, VP3, LT, or st respectively)-specific versus MOPP- and sum-antigen-specific IFN γ -, IL-2- and TNF α -producing CD4+ T-cells, respectively. Figure B shows the median frequencies with inter-quartile range of BKV-specific CD8+ T-cells that produce IFN γ upon VP1-, VP2-, VP3-, LT-, st-stimulation in comparison with stimulation by MOPP and sum and after background subtraction. Stimulation by MOPP showed significantly higher incidence of patient with detectable BKV-specific CD8+ T-cells and significantly higher frequencies of BKV-specific IFN γ + CD8+ T-cells (*p < 0.05; ** p < 0.01; *** p < 0.001). The higher percentage of patients with detectable IL-2 and TNF α -producing BKV-specific T-cells obtained from the calculated theoretical sum versus MOPP reflects the amino acid overlap within regulatory proteins LT and st and structural proteins VP1, VP2, VP3, respectively.

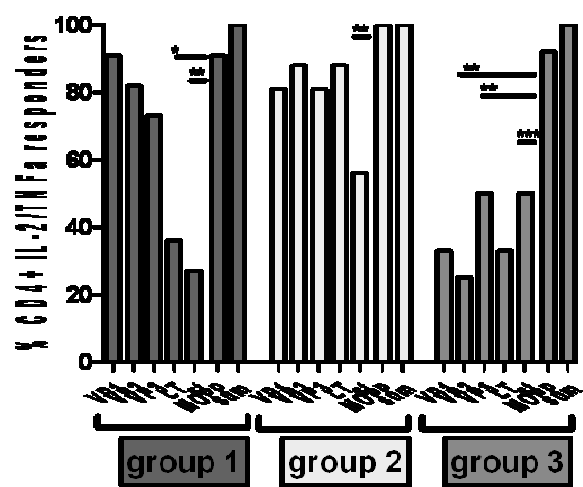
A



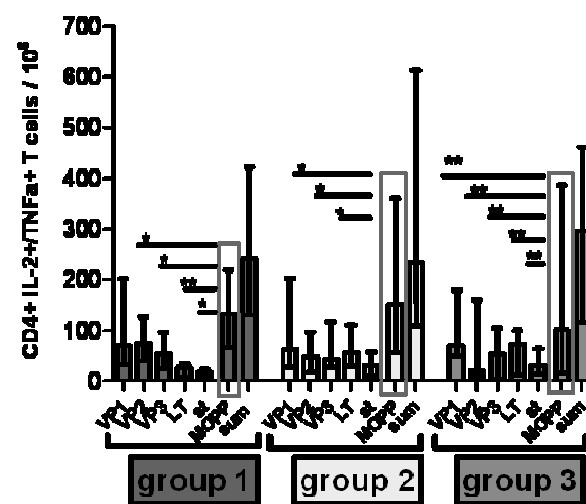
B



C



D

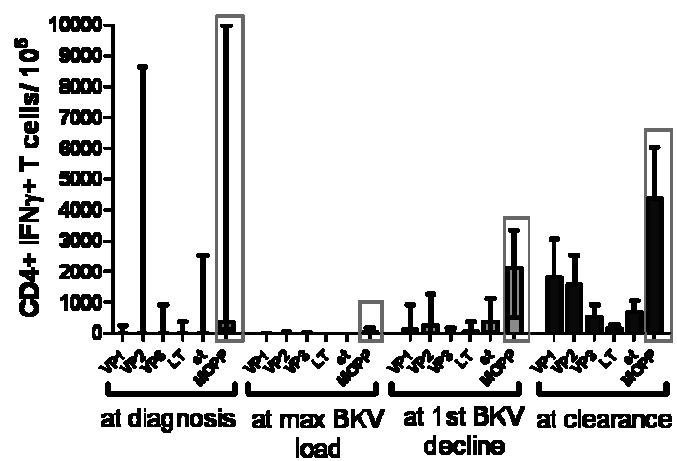


Supplemental figure 3

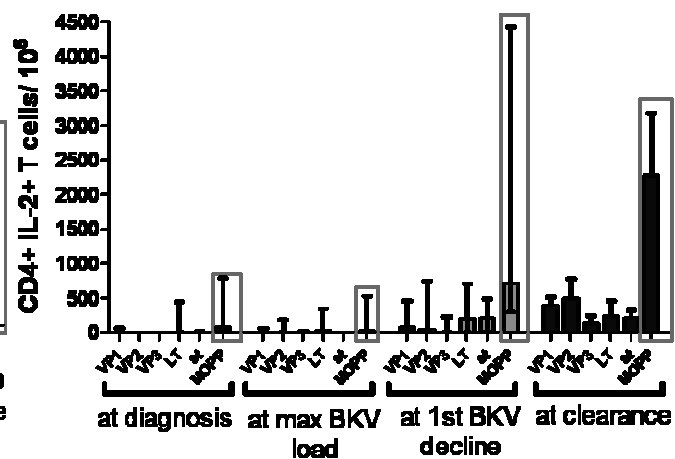
Supplemental Figure S3. Incidence of multifunctional CD4⁺ triple IFN γ /IL-2/TNF α (A) and double IL-2/TNF α (C) responders and magnitude of total IFN γ +/IL-2+/TNF α + (B) and IL-2+/TNF α + (D) CD4⁺ T-cell responses in different patient groups

Figures A, C demonstrate the percentage of KTRs with detectable SOPP (VP1, VP2, VP3, LT, or st, respectively)-specific versus MOPP- and sum-specific IFN γ +/IL-2+/TNF α + and IL-2+/TNF α + CD4⁺ T-cells, respectively. Figure B, D show the median frequencies with inter-quartile range of BKV-specific CD4⁺ T-cells that produce IFN γ /IL-2/TNF α and IL-2/TNF α upon SOPP (VP1, VP2, VP3, LT, or st, respectively)-specific stimulation in comparison with stimulation by MOPP and sum and after background subtraction. Patients with a history of fast BKV clearance had a significantly higher frequencies of BKV-specific polyfunctional IFN γ /IL-2/TNF α -producing CD4⁺ T cells compared to patients with a history of severe long-lasting BKV infection (*p < 0.05; ** p < 0.01; *** p < 0.001). The higher frequency of double and triple cytokine producing T-cells obtained from the calculated theoretical sum versus MOPP reflects the amino acid overlap within regulatory proteins LT and st and structural proteins VP1, VP2, VP3, respectively.

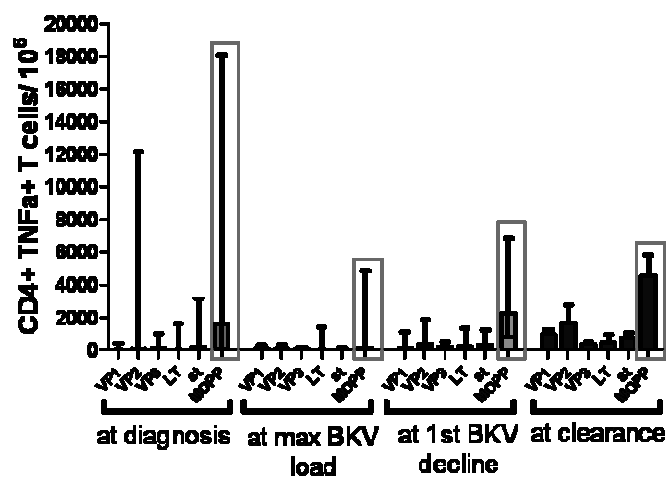
A



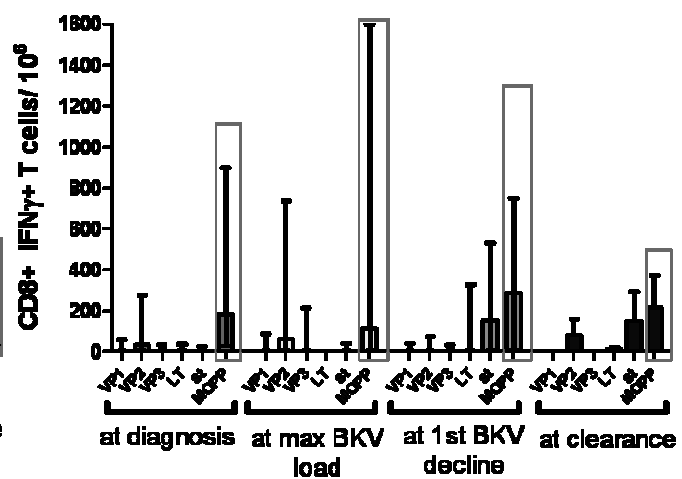
B



C



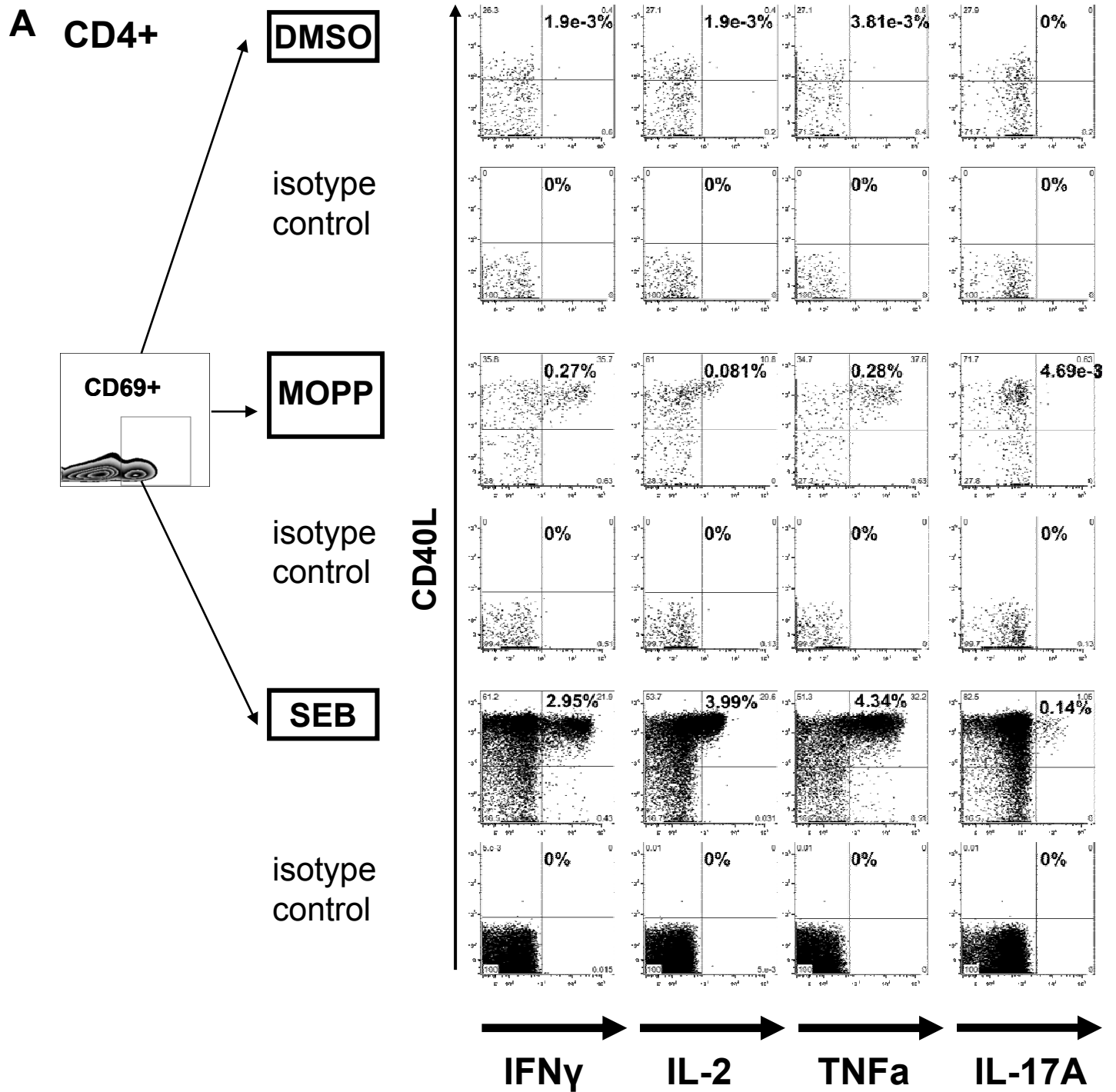
D



Supplemental figure 4

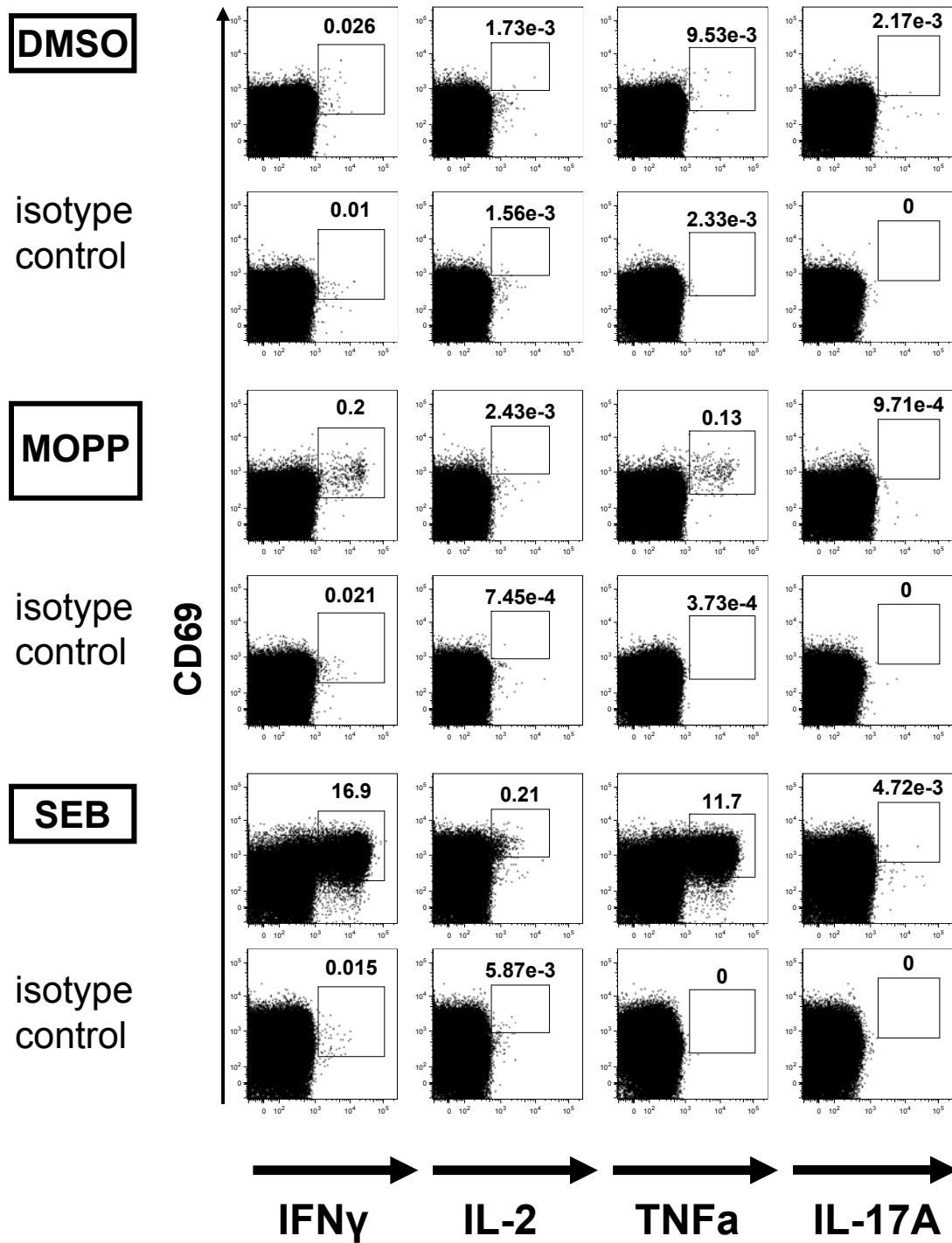
Supplemental Figure S4. Kinetics of total IFN γ + (A), IL-2+ (B) and TNF α + (C) CD4+ and IFN γ + (D) CD8+ T-cell responses in KTRs during the clinical course of BKV re-activation

Figures A, B, C, D show the median frequencies with inter-quartile range of BKV-specific CD4+ and CD8+ T cells that produce IFN γ , IL-2 and TNF α , respectively upon VP1-, VP2-, VP3-, LT-, st- single stimulation (SOPP) in comparison with MOPP stimulation and after background subtraction at the time of diagnosis, maximum BKV load, first BKV decline and clearance. MOPP stimulation approach enabled much more efficient monitoring of BKV-specific cellular kinetics during the clinical course of BKV reactivation compared to SOPP stimulations.



Supplemental figure 5A

B CD8+



Supplemental figure 5B

Supplemental Figure S5. Isotype controls for CD4+ (A) and CD8+ (B) T-cell responses

Gates were set on CD3+ lymphocytes, doublets and dead cells were discriminated. CD4+ (A) and CD8+ (B) T-cells were subdivided. CD69 was used as an early activation marker and CD40L - as a marker for T-helper cells which have been recently activated. Subsequent multiparameter flow cytometric analysis was performed according to the expression of IFN γ , IL-2, TNF α and IL-17A. SEB was used as positive control and DMSO as negative control. CD69+ gating strategy was chosen as a representative sample after SEB stimulation. Isotype-matched control antibodies were used to distinguish non-specific ("background") stainings.